Journal of the American College of Cardiology
© 2009 by the American College of Cardiology Foundation
Published by Elsevier Inc.

Vol. 53, No. 17, 2009
ISSN 0735-1097/09/$36.00
doi:10.1016/j.jacc.2008.12.056

Thin-Walled Microvessels in Human Coronary Atherosclerotic Plaques Show Incomplete Endothelial Junctions

Relevance of Compromised Structural Integrity for Intraplaque Microvascular Leakage

Judith C. Sluimer, PhD,* Frank D. Kolodgie, PhD,† Ann P. J. J. Bijnens, PhD,* Kimberly Maxfield, BSc,† Erica Pacheco, MSc,† Bob Kutys, MSc,† Hans Duimel, BSc,* Peter M. Frederik, PhD,* Victor W. M. van Hinsbergh, PhD,‡ Renu Virmani, MD, PhD,† Mat J. A. P. Daemen, MD, PhD*

Maastricht and Amsterdam, the Netherlands; and Gaithersburg, Maryland

Objectives This study sought to examine the ultrastructure of microvessels in normal and atherosclerotic coronary arteries and its association with plaque phenotype.

Background Microvessels in atherosclerotic plaques are an entry point for inflammatory and red blood cells; yet, there are limited data on the ultrastructural integrity of microvessels in human atherosclerosis.

Methods Microvessel density (MVD) and ultrastructural morphology were determined in the adventitia, intima-media border, and atherosclerotic plaque of 28 coronary arteries using immunohistochemistry for endothelial cells (*Ulex europeaus*, CD31/CD34), basement membrane (laminin, collagen IV), and mural cells (desmin, alpha-smooth muscle [SM] actin, smoothelin, SM1, SM2, SMemb). Ultrastructural characterization of microvessel morphology was performed by electron microscopy.

Results The MVD was increased in advanced plaques compared with early plaques, which correlated with lesion morphology. Adventitial MVD was higher than intraplaque MVD in normal arteries and early plaques, but adventitial and intraplaque MVD were similar in advanced plaques. Although microvessel basement membranes were intact, the percentage of thin-walled microvessels was similarly low in normal and atherosclerotic adventitia, in the adventitia and the plaque, and in all plaque types. Intraplaque microvascular endothelial cells (ECs) were abnormal, with membrane blebs, intracytoplasmic vacuoles, open EC-EC junctions, and basement membrane detachment. Leukocyte infiltration was frequently observed by electron microscopy, and confirmed by CD45RO and CD68 immunohistochemistry.

Conclusions The MVD was associated with coronary plaque progression and morphology. Microvessels were thin-walled in normal and atherosclerotic arteries, and the compromised structural integrity of microvascular endothelium may explain the microvascular leakage responsible for intraplaque hemorrhage in advanced human coronary atherosclerosis. (J Am Coll Cardiol 2009;53:1517–27) © 2009 by the American College of Cardiology Foundation

Atherosclerotic plaque rupture and symptomatic coronary disease are closely related to the presence of intraplaque and adventitial angiogenesis (1,2). Intraplaque microvessels are surrounded by macrophages and red blood cells, and hemorrhage, secondary cholesterol accumulation, and inflammation in atherosclerotic plaques are associated with plaque rupture (3–6).

Macrophages and red blood cells are thought to extravasate from the intraplaque microvessel lumen into the plaque tissue (7). Microvascular structural integrity determines

From the *Maastricht University Medical Center, Department of Pathology, CARIM, Maastricht, the Netherlands; †CVPath, Gaithersburg, Maryland; and the ‡VU Medical Center, Department of Physiology, ICAR-VU, Amsterdam, the Netherlands. Research was partly supported by a travel grant from the Netherlands Organization for Scientific Research (Dr. Sluimer) and a grant from the National Institutes of Health (RO1HL071148-05 to Dr. Virmani). Drs. Daemen and van Hinsbergh participate in the European Vascular Genomics Network (http://www.evgn.org), a Network of Excellence supported by the European Community's Sixth Framework Program for Research Priority 1 (contract LSHM-CT-2003-503254).

Manuscript received June 2, 2008; revised manuscript received December 3, 2008, accepted December 8, 2008.

JACC Vol. 53, No. 17, 2009
April 28, 2009:1517–27

Abbreviations and Acronyms

EC = endothelial cell
E-FA = thick fibrous cap atheroma with an early core
IEL = internal elastic lamina
IM = intima-media
IT = intimal thickening, normal
L-FA = thick fibrous cap atheroma with late necrotic core
MVD = microvessel density
PIT = pathological intimal thickening
SM = smooth muscle
SMA = smooth muscle actin
SMC = smooth muscle cell
TCFA = thin fibrous cap atheroma
VEGF = vascular endothelial growth factor

microvessel leakage, but a comprehensive analysis of intraplaque microvessel structure is lacking. Physiological angiogenesis starts with increased microvessel permeability and matrix degradation, followed by endothelial cell (EC) migration and/or proliferation. The resulting thin-walled, permeable sprouts are matured by basement membrane formation and mural cell recruitment. Research on pathological angiogenesis in tumors has established features of microvascular leakage (8). The majority of tumor microvessels are endothelial-lined tubes without coverage by basement membrane or mural cells, and these thin-walled structures are prone to leakage (8–10). The possible fragility of plaque microvessels corroborates the suggested leakage of macrophages and red blood cells.

Microvascular leakage is also characterized by a disruption of endothelial integrity, which is normally maintained by intercellular junctions (11). Microvessels with aberrant endothelial junctions show microvascular leakage (9). Based on the findings in physiological and pathological angiogenesis, we hypothesize that the structural integrity of plaque microvessels in human atherosclerosis is incomplete, possibly explaining the inflammatory infiltration and red blood cell extravasation.

See page 1528

Therefore, microvessel density (MVD) and ultrastructure were studied in human atherosclerotic plaques of varying morphology and in normal coronary arteries using quantitative analysis of MVD, endothelial morphology and integrity, and mural cell and basement membrane presence by light and electron microscopy.

Materials and Methods

Tissue collection. Atherosclerotic coronary arteries (n = 28) were obtained at autopsy from 28 sudden-death donors (Table 1). Collection, storage, and use of tissue and patient data were performed in agreement with institutional ethical guidelines. Samples were processed and classified, based on plaque morphology, as intimal thickening (IT) (normal), pathological intimal thickening (PIT), a thick fibrous cap atheroma with an early necrotic core (E-FA) or a late necrotic core (L-FA), a thin fibrous cap atheroma (TCFA), or a ruptured plaque, as described previously (12). Samples were included in the study without any pre-selection based on angiogenesis.

Table 1 Demographics and Clinical Characteristics

	Frequency, % (n)*
Age (yrs)†	55.5 (2.8)
Male	89 (25)
Ethnicity	
Caucasian	71 (21)
African-American	25 (7)
Hypertension	26 (6)
Hypercholesterolemia	9 (2)
Smoking	30 (7)
Alcohol use	22 (5)
Statin therapy	0 (0)
Type 2 diabetes mellitus	9 (2)
History of cardiovascular disease	17 (4)

*Unless stated otherwise. †Mean (SEM).

Immunohistochemistry. Immunohistochemistry was performed on paraffin-embedded sections with IT (n = 5), PIT (n = 5), E-FA (n = 4), L-FA (n = 5), TCFA (n = 5), or ruptured plaques (n = 4). Serial sections were stained with primary antibodies (Table 2) against macrophages (CD68), endothelial cells (*Ulex aeropaeus* lectin-1, CD31/CD34 cocktail), mural cells (alpha smooth muscle actin [αSMA], desmin), smooth muscle (SM) differentiation markers (smoothelin, SM myosin heavy chain SM1, SM2, and nonmuscle-type MHC SMemb), basement membrane (laminin, collagen IV), leukocytes (CD45RO), and mast cells (mast cell tryptase). Staining was visualized using 3,3′-diaminobenzidine tetrachloride (DAKO, Glostrup, Denmark) tinted with 0.04% nickel chloride (Sigma-Aldrich, St. Louis, Missouri). Evaluation of the staining pattern in control tissue, in which marker expression had previously been described, and omission of a primary antibody served as specificity controls.

Quantitative morphometry. Histological and morphometric analysis of atherosclerosis was performed as described elsewhere (13). Maximal intimal thickness was taken as the maximal distance perpendicular from the plaque surface to the internal elastic lamina (IEL). The maximal percentage of artery stenosis was calculated as: (IEL perimeter − lumen perimeter)/(IEL perimeter) × 100.

Microvessels were quantified in hotspots (≥3 microvessels) using ×200 fields of 3 regions: the adventitia, intima-media (IM) border, and intraplaque region (close to the necrotic core and away from the media) using image-processing software (IVision, Scanalytics, Rockville, Maryland). Adventitial microvessels were quantified using $ULEX^+$ microvessels in 1 hotspot per quadrant, whereas $CD31^+CD34^+$ microvessels in the IM border and intraplaque regions were counted in ≤3 hotspots. The IM border was limited to twice the thickness of the normal

Table 2 Immunohistochemical Methods

Antibody	Company, Product Code	Expression	Dilution	Incubation	Antigen Retrieval	Blocking	Detection
CD68	Dako, M0814	Macrophage	1:300	O/N	EDTA pH = 8	Pre-AB block	Powervision-HRP
Ulex europeaus lectin-1	Vector Laboratories, L-1060	Endothelial cell	1:400	1 h, RT	None	10% horse serum	LSAB-HRP
CD31/CD34	Dako, M0823/Monosan, MON1164	Endothelial cell	1:50/1:200	1 h, RT	EDTA pH = 8	Pre-AB block	Powervision-HRP
Desmin	Sigma, #1033	Mural cell	1:50	O/N	EDTA pH = 8	Pre-AB block	Powervision-HRP
αSMA	Dako, M0851	Mural cell	1:400	1 h, RT	None	None	Powervision-HRP ABC-AP (double*)
Smoothelin	Monosan, MON 2094	SM differentiation	1:10	1 h, RT	Cryosection	Pre-AB	Powervision-HRP
SM1	Seigaku, #7599	SM differentiation	1:800	1 h, RT	Cryosection	Pre-AB	Powervision-HRP
SM2	Seigaku, #7601	SM differentiation	1:800	1 h, RT	Cryosection	Pre-AB	Powervision-HRP
SMemb	Seigaku, #7602	SM differentiation	1:800	1 h, RT	Cryosection	Pre-AB	Powervision-HRP
Collagen IV	Eurodiagnostica, PC02233	Basement membrane	1:4,000	1 h, RT	Pepsin	Pre-AB block	Powervision-HRP
Laminin	Neomarkers, 86103	Basement membrane	1:100	1 h, RT	Protease 8	Pre-AB block	Powervision-HRP
CD45	Dako, M0701	Leukocyte	1:500	1 h, RT	None	None	Powervision-HRP
Mast cell tryptase	Dako, M7052	Mast cells	1:1,000	1 h, RT	None	None	Powervision-HRP

*Double, double staining with *Ulex europeaus*.

AB = antibody blocking; ABC-AP = alkaline phosphatase conjugated avidin-biotin complex (Vector Laboratories, Burlingame, California); EDTA = 1 mmol/l ethylene diaminetetraacetic acid; LSAB-HRP = LSAB Strep-avidin horseradish peroxidase conjugated (Dako, Glostrup, Denmark); O/N = overnight; Pepsin = 0.1% pepsin in 0.1N HCl; Powervision-HRP = horseradish peroxidase conjugated Powervision goat antimouse/rabbit/rat antibody (immunologic); Pre-AB block = Powervision pre-antibody blocking reagent (Immunologic, Duiven, the Netherlands); Protease 8 = 0.05% protease 8 (Sigma-Aldrich, St. Louis, Missouri) in 0.05M Tris/0.01M CaCl2, pH = 7.6; αSMA = alpha smooth muscle actin; RT = room temperature; SM = smooth muscle.

media. MVD was computed as the total number of vessels/total area, and mural cell coverage as αSMA^+ microvessel/total microvessel. When mural cells were present, mural cell layers were differentiated as single or multiple layers. The average across hotspots of each measurement was computed per region.

Electron microscopy. Coronary artery sections with normal intima (n = 1) or advanced plaques (FA n = 2; ruptured n = 4) were obtained from 7 additional donors (age 60 ± 6 years, 6 male, 5 Caucasian and 2 African-American). Tissue fragments of approximately 1 mm^3 were fixed overnight in 2.5% glutaraldehyde (Ted Pella, Redding, California), post-fixed in 1% osmium tetroxide solution, dehydrated, and embedded in epoxy resin. Semi-thin (1 μm) serial sections were stained with toluidine blue to localize microvessels. Ultra-thin sections (70 to 90 nm) were mounted on Formvar (1595 E, Merck, Amsterdam, the Netherlands)-coated 75 mesh copper grids, and counterstained with uranyl acetate and lead citrate before analysis on a Philips CM100 transmission electron microscope (Philips, Eindhoven, the Netherlands).

Statistical analysis. The overall difference between plaque types in terms of plaque morphology, MVD, and mural cell coverage was tested using a nonparametric Kruskal-Wallis test, followed by a Mann-Whitney *U* test to determine which plaque types were different. A 2-tailed Fisher exact test was used to test the frequency distribution of concentric/eccentric morphology between plaque types. The Spearman nonparametric correlation coefficient ρ was calculated for plaque morphology, MVD, and mural cell coverage (version 12.0, SPSS Inc., Chicago, Illinois). Results were considered statistically different when $p < 0.05$.

Results

Plaque morphology changed with plaque progression. Plaque area, maximal intimal thickness, stenosis, necrotic core, macrophage, and calcification significantly increased with progression of atherosclerosis (Figs. 1A to 1F). Ruptured plaques were more often concentric than eccentric as compared with PIT, early, and late FA plaque stages (Table 3). The relationship between plaque composition and plaque stage were as reported in the literature, indicating that a representative coronary plaque selection had been collected.

MVD increased with early plaque progression and plaque morphology. Angiogenesis in atherosclerotic plaques was present in 3 regions: the adventitia, IM border, and intraplaque region (Figs. 2A to 2D). MVD in the adventitia ($p = 0.03$), IM border ($p = 0.01$), and intraplaque region ($p = 0.025$) (Figs. 2E to 2G) significantly increased with plaque progression. A significant difference in MVD was observed between normal arteries or early plaque stages (PIT) and advanced plaques (FA and ruptured) in all arterial wall regions. However, MVD in late core fibroatheromas did not differ from that in ruptured plaques (Figs. 2E to 2G). Likewise, plaque morphometry was generally similar between late core fibroatheromas, TCFAs, and ruptured plaques (Fig. 1). The MVD was significantly higher in concentric plaques, presumably because advanced plaques, with concomitant higher MVD, were more often concentric (Fig. 2H).

In advanced plaques, the MVD was similar in all vessel wall regions, whereas in early plaques, adventitial MVD was significantly higher than IM border and intraplaque MVD

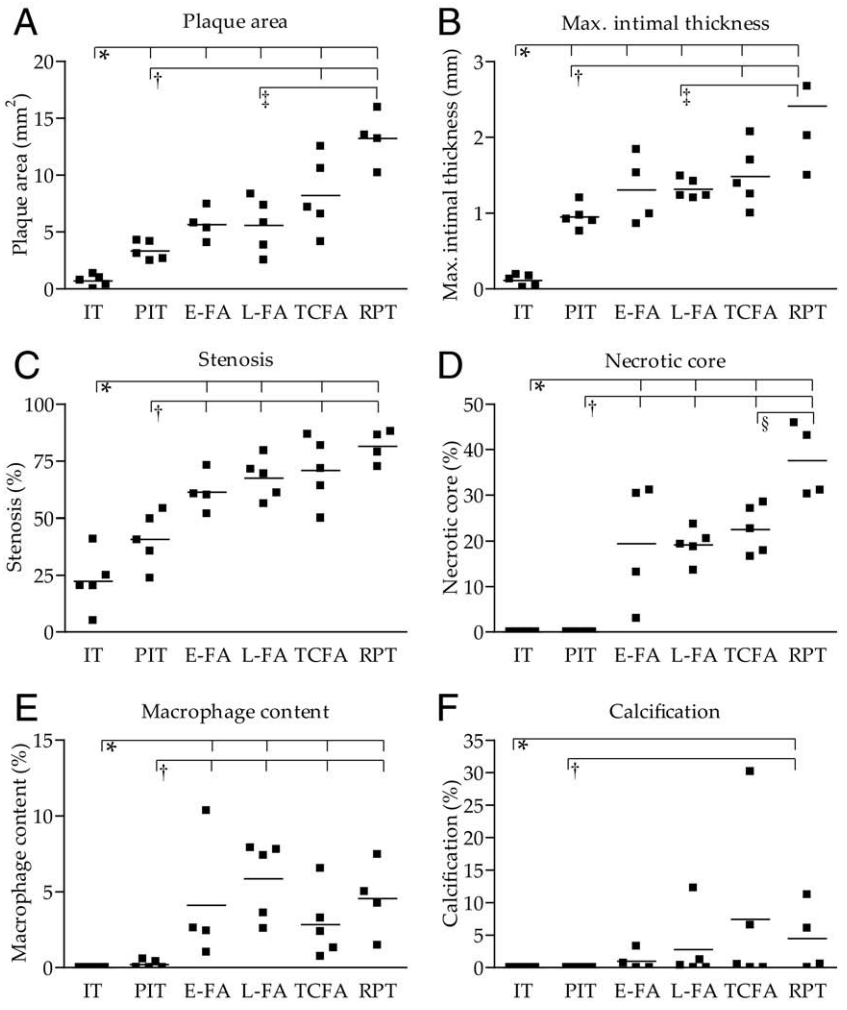

Figure 1 **Atherosclerotic Plaque Morphology in Normal and Atherosclerotic Coronary Arteries**

(A) Plaque area, **(B)** maximal intimal thickness, **(C)** stenosis, **(D)** necrotic core content, **(E)** macrophage content, and **(F)** calcification content in normal coronary artery and various coronary plaque types. *$p < 0.05$ versus IT. †$p < 0.05$ versus PIT. ‡$p < 0.05$ versus L-FA. §$p < 0.05$ versus TCFA. E-FA = thick fibrous cap atheroma with an early necrotic core; IT = normal intimal thickening; L-FA = thick fibrous cap atheroma with a late necrotic core; PIT = pathological intimal thickening; RPT = ruptured plaque; TCFA = thin fibrous cap atheroma.

(Figs. 2E to 2G). In addition, the trend of increasing adventitial MVD with plaque stage did not correlate with the intraplaque and IM border MVD trends ($\rho = 0.30$, p = 0.140; and $\rho = 0.35$, p = 0.056, respectively). The MVD magnitude and trends were similar in IM border and intraplaque regions ($\rho = 0.44$, p = 0.028). Microvessels were observed invading from the adventitia, through the medial elastic lamina breaches into the plaque, in line with previous studies showing the adventitia as the origin of microvessel sprouting (Figs. 3A and 3B) (2,14). Together, these results suggest that the onset of adventitial microvessels in atherogenesis preceded that in the IM border and intraplaque regions.

The MVD in all 3 regions correlated significantly with plaque morphology (Table 4). However, this effect was no longer observed after stratification for plaque stage. No association was observed between MVD and plaque calcification (Table 4).

Table 3 **Frequencies of Concentric Vessel Morphology in Different Plaque Types**

Plaque Type	Concentric, % (n)
PIT*	20 (1)
E-FA	40 (2)
L-FA	40 (2)
TCFA	80 (4)
Rupture	100 (5)

*$p < 0.05$ versus rupture.

E-FA = thick fibrous cap atheroma with an early necrotic core; L-FA = thick fibrous cap atheroma with a late necrotic core; PIT = pathological intimal thickening; TCFA = thin fibrous cap atheroma.

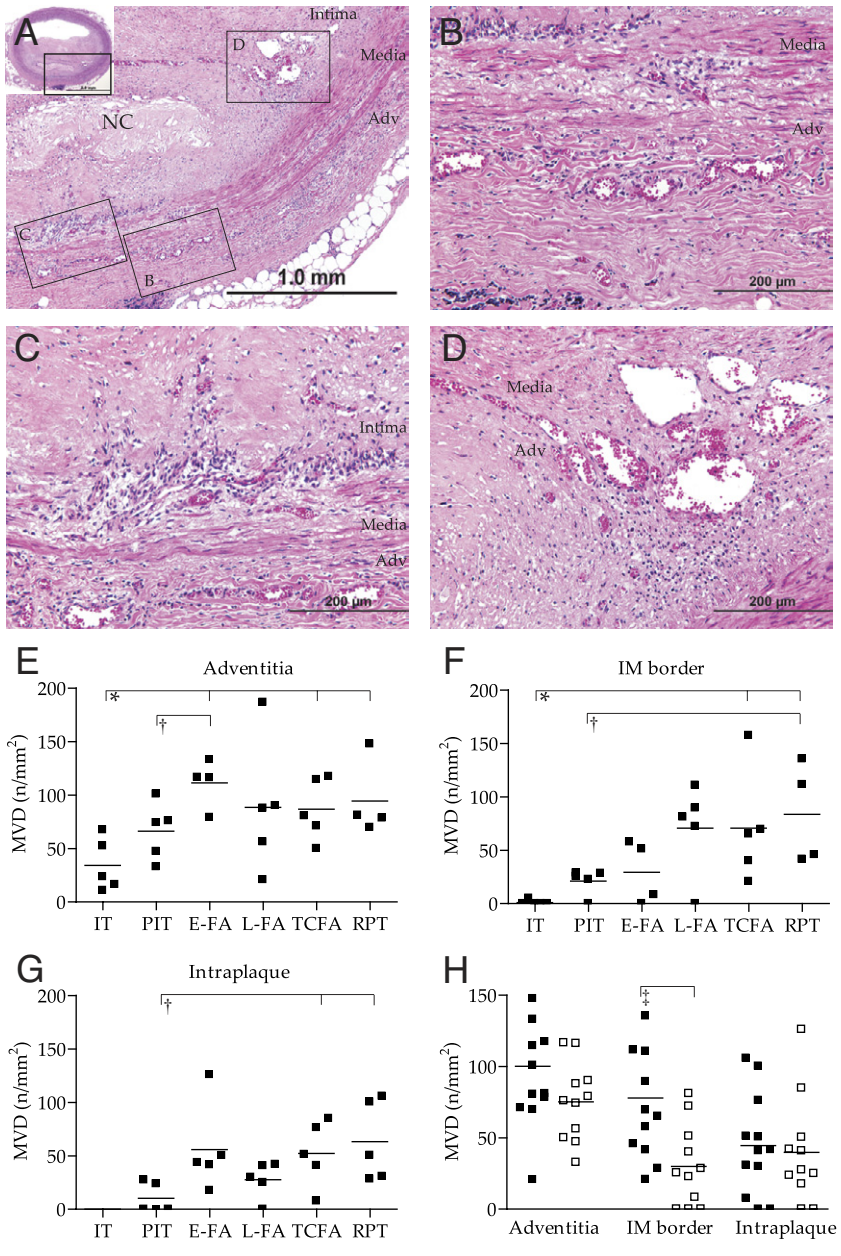

Figure 2 **MVD Increases With Atherosclerotic Progression**

(A) Detail of hematoxylin and eosin–stained coronary artery with thick cap fibroatheroma (necrotic core [NC]); **inset** shows entire coronary artery. **Boxed regions B to D** illustrate the regions of interest and correspond to **(B)** showing microvessels in the adventitia (ADV), **(C)** intima-media (IM) border, and **(D)** in the intraplaque region. Mean microvessel density (MVD) was quantified in **(E)** adventitia, **(F)** the IM border, and **(G)** the intraplaque region, and increased with progression. **(H)** MVD was higher in concentric **(solid squares)** than in eccentric **(open squares)** plaques. *$p < 0.05$ versus IT. †$p < 0.05$ versus PIT. ‡$p < 0.05$ eccentric versus concentric. Abbreviations as in Figure 1.

Basement membrane is intact, but mural cell coverage is low in normal and atherosclerotic coronary arteries. Immunohistochemistry of basement membrane (laminin, collagen IV) and mural cells (αSMA, desmin) was performed to establish microvessel structure in normal and atherosclerotic coronary arteries. Microvessels in all regions were generally surrounded by laminin, and some also by collagen IV (Figs. 3C and 3D), indicating that the microvessel basement membrane was present and intact. In contrast, mural cells were infrequently present (Figs. 3E to 3H).

Mural cells surrounding microvessels may be pericytes or smooth muscle cells (SMCs), a distinction mostly based on whether they share a basement membrane with the ECs or not. However, morphology and marker expression may vary with the tissue and/or pathology, hindering the identification of pericytes or SMCs (15). We therefore did not

JACC Vol. 53, No. 17, 2009
April 28, 2009:1517–27

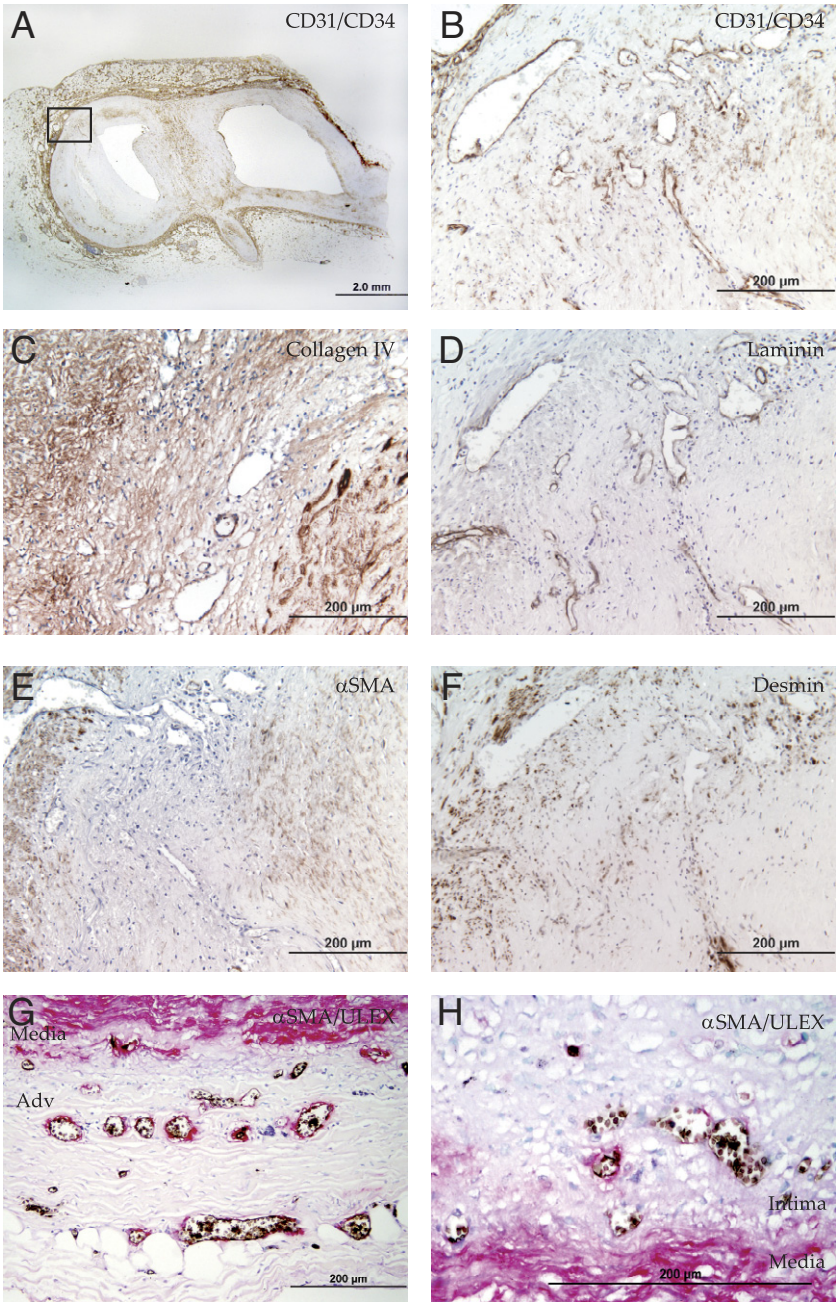

Figure 3 **Basement Membrane and Mural Cell Coverage in Normal and Atherosclerotic Coronary Arteries**

(A) Coronary fibroatheroma stained with CD31/CD34 cocktail. **Boxed region** indicates origin of **(B)** $CD31^{+}CD34^{+}$ microvessels run from the adventitia through the media into the plaque. Adjacent section stained with **(C)** collagen IV or **(D)** laminin, showing intact microvessel basement membrane in the adventitia, intima-media (IM) border, and plaque. **(E)** Adjacent section stained with alpha smooth muscle actin (SMA), showing mostly αSMA^{-} microvessels in the adventitia, IM border, and plaque. **(F)** Adjacent section stained with desmin shows some $desmin^{+}$ microvessels in the adventitia, IM border, and intraplaque region. **(G)** Adjacent section double-stained with lectin-1 **(black)** and αSMA **(red)** shows infrequent mural cell coverage in the adventitia and **(H)** in the IM border. Abbreviations as in Figure 2.

distinguish between mural cell types. On histology, the single-layered or multilayered mural cells most likely represented vascular SMCs, although electron microscopy also showed single-layered pericytes sharing basement membrane with EC. Thus, αSMA and desmin-expressing cells were encountered surrounding arterial wall microvessels, but at low percentages (Figs. 3E to 3H). Moreover, well-established markers of SMC differentiation SM1 and SM2 were also infrequently expressed, whereas microvessels remained mostly negative for SMemb or the late differentiation marker, smoothelin (data not shown). Unexpectedly, the percentage of thin-walled microvessels was no different between normal and atherosclerotic arteries, or

Table 4 Spearman ρ Correlation Coefficients of Microvessel Density and Plaque Morphology

	Microvessel Density		
	Adventitia	IM Border	Intraplaque
Plaque area	0.53†	0.785†	0.63†
Maximum intimal thickness	0.54†	0.71†	0.68†
Stenosis	0.60†	0.70†	0.47*
Necrotic core content	0.57†	0.52†	0.51†
Macrophage content	0.49†	0.58†	0.57†
Calcification content	0.35	0.65†	0.37

*$p < 0.05$. †$p < 0.01$.

between the different plaque types (Figs. 4A to 4C). If present, mural cell layers (single or multiple) did not differ between plaque types either (Figs. 4D to 4F). Also, no difference in mural cell coverage was observed between different vessel wall regions, nor was mural cell coverage correlated with plaque morphology.

Plaque microvessels show abnormal EC morphology, aberrant EC junctions, and leukocyte adherence. Because microvascular leakage is also characterized by a disruption of endothelial integrity, interendothelial junctions were studied using electron microscopy. Interendothelial junctions were intact in adventitial microvessels in a nondiseased coronary artery (Figs. 5A and 5B). Junctions of intraplaque microvessels were quantitatively analyzed in atherosclerotic coronary arteries with advanced fibroatheromas and ruptured plaques. Although an intact basement membrane was generally observed (Figs. 5C to 5F), interendothelial contact was incomplete or completely absent in 76% of analyzed microvessels and endothelial junctions (Fig. 5D, Table 5). Thus, endothelial integrity was severely compromised. In addition, EC morphology frequently represented an activated, dysfunctional status, characterized by blebbing and spike-like protrusions of the cell membrane. Also, numerous intracytoplasmic vacuoles, a sign of in-

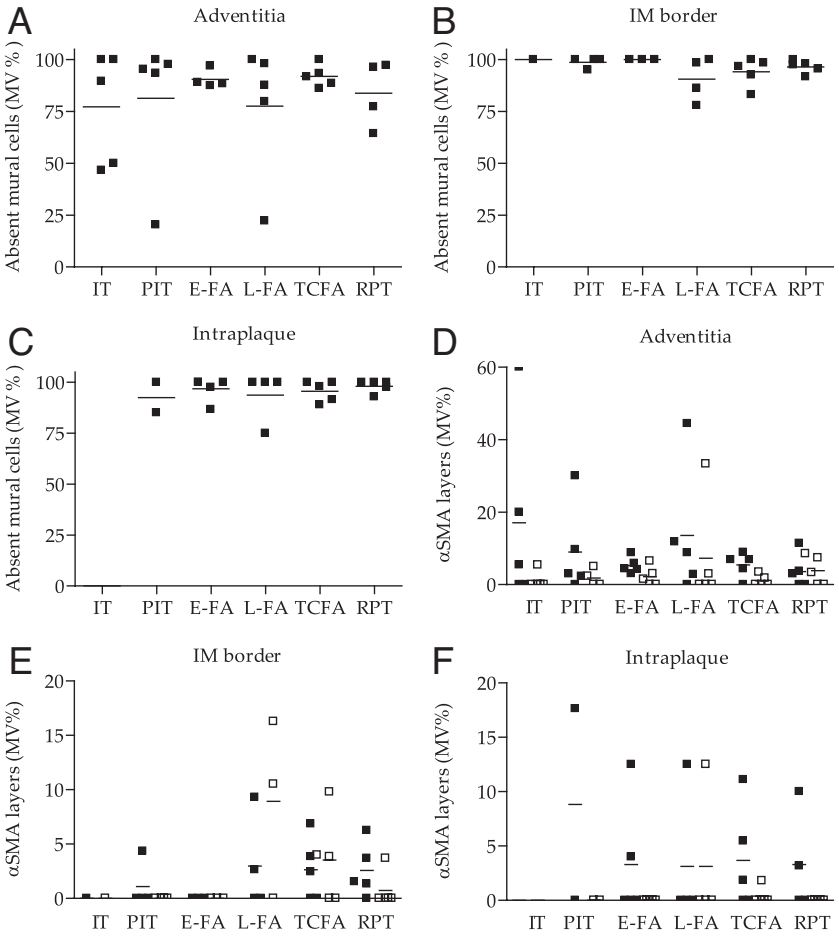

Figure 4 Quantification of Mural Cell Coverage in Various Plaque Types

Mural cell coverage was low in the **(A)** adventitia, **(B)** intima-media (IM) border, and **(C)** intraplaque region of both normal and atherosclerotic coronary arteries. **(D)** Percentage of microvessels with single **(solid squares)** and multiple **(open squares)** mural cell layers in adventitia, **(E)** intima-media (IM) border, and **(F)** intraplaque region. All p values > 0.05. IT = normal intimal thickening; PIT = pathological intimal thickening; other abbreviations as in Figure 1.

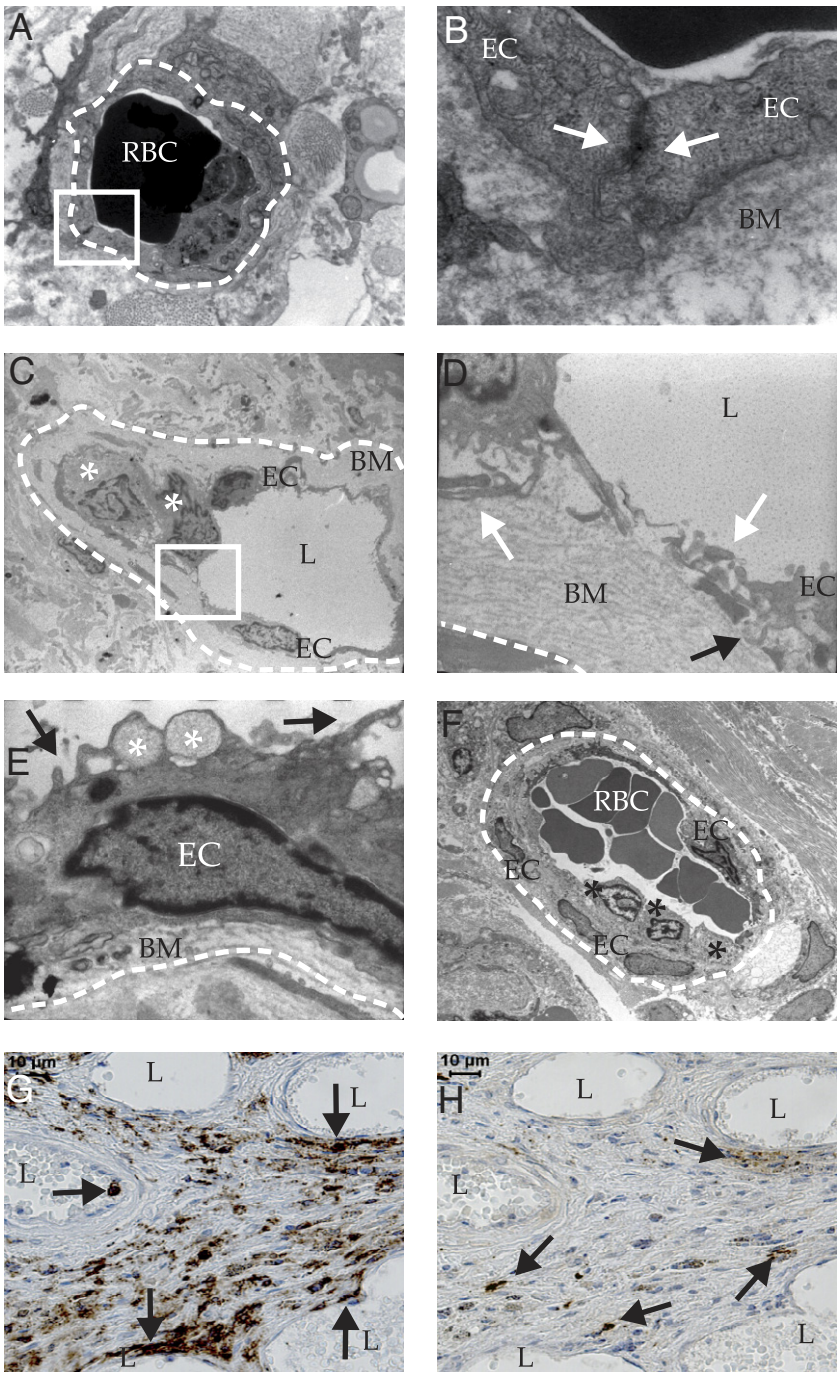

Figure 5 **Intraplaque Microvessels Show Abnormal EC Morphology, Aberrant Junctions, and Leukocyte Infiltration as Shown by EM**

(A) Ultrastructure of an adventitial microvessel (**dashed line** indicates circumference) in a nondiseased coronary artery with luminal red blood cells (RBCs) (electron microscopy [EM], ×8,000). **(B)** Magnification of the **boxed region in A** of microvessel with intact basement membrane (BM) and interendothelial junction indicated by close contact **(white arrows)** between endothelial cells (ECs) (×20,000). **(C)** Ultrastructure of intraplaque microvessel with leukocytes **(white asterisks)** (×650). **(D)** Magnification of the **boxed region in C** showing aberrant inter-EC junction **(white arrows)** and basement membrane detachment **(black arrow)** (×4,600). **(E)** Dysfunctional EC ultrastructure in an intraplaque microvessel (×6,300): membrane blebs **(black arrow)** and intracytoplasmic vacuoles **(white asterisk)**. **(F)** Leukocytes **(asterisks)** adhering to intraplaque microvessel endothelium (×460). **(G)** Immunohistochemistry shows $CD45^+$ cells in and near microvessels **(arrows)**. **(H)** Immunohistochemistry showing mast cell tryptase-positive cells at larger distance from microvessels **(arrows)**. L = lumen.

Table 5 Electron Microscopy Analysis of Endothelial Cell Morphology, Junctions, and Leukocyte Infiltration in Intraplaque Microvessels

	Occurrence (n)
Microvessels with all junctions intact	24% (8)
Microvessels with >1 open junction	76% (19)
Microvessels with all junctions open	33% (8)
Total open junctions	59% (34)
Basement membrane detachment	42% (11)
Leukocyte infiltration	50% (13)

creased secretory capacity, were observed (Fig. 5E). Moreover, membrane detachment was frequently observed (Fig. 5E, Table 5). In addition, cells were adhering to the microvessel lumen and infiltrating into the plaque in 50% (n = 13) of microvessels (Figs. 5C and 5F, Table 5). These were identified as monocytes, based on nuclear morphology, and CD45RO (Fig. 5G) and CD68 (not shown) immunoreactivity. Mature mast cells were frequently present in the plaque in the proximity of microvessels (Fig. 5H). As mast cell tryptase is only expressed by tissue-resident, matured mast cells, it cannot fully be excluded that immature mast cells adhere to the luminal side of plaque microvessels. Nevertheless, the nuclear morphology and CD68 expression indicate that adhering cells are monocytes (Figs. 5C and 5F). Thus, abnormal EC morphology and junctions were associated with monocyte/macrophage infiltration.

Discussion

The association of MVD and microvessel ultrastructure with coronary atherosclerosis plaque type and morphology was determined using structural parameters related to microvascular leakage: basement membrane and mural cell coverage and endothelial junction integrity. MVD was increased in fibroatheromas and ruptured plaques compared with normal and pathological intimal thickening, and was associated with plaque morphology. Microvessels were observed meandering from the adventitia through the media into the atherosclerotic plaque. The adventitia is the origin of >95% of plaque microvessels, as comprehensively shown by 3-dimensional angiography and serial sectioning (2,14). Other reports confirmed that the onset of adventitial angiogenesis preceded intraplaque angiogenesis (16) and coincided with the onset of atherosclerosis (17).

Thus, angiogenesis and atherogenesis develop in close conjunction. Intraplaque microvessels are rare in small animal models of atherosclerosis (18), whereas they are abundant in human plaques (1,2,16,19). This suggests that microvessels need not be abundantly present to allow initiation and development of atherosclerosis. The growth of intraplaque microvessels may thus simply be a physiological reaction. Regardless of whether microvessel plaque content is merely a reaction to plaque growth, growing evidence suggests that the abnormal microvessel structure may be involved in atherosclerotic plaque destabilization.

Microvessels in our human samples with coronary atherosclerosis commonly showed incomplete mural cell coverage (Figs. 3E and 3F) and a compromised structural integrity accompanied by extensive macrophage infiltration (Figs. 5C to 5G). Contrary to our expectations, mural cell coverage was infrequent even in normal coronary arteries, and was similar in all plaque types and vessel wall regions. Hence, incomplete mural cell coverage cannot explain microvascular and subsequent intraplaque leakage. Recent reports also described intraplaque angiogenesis lacking mural cell coverage in atherosclerotic femoral (20) and carotid arteries (21,22). Plaques of symptomatic patients showed significantly fewer microvessels covered with SMCs than those of asymptomatic patients (21), in contrast to our study of sudden death victims. Unfortunately, these studies did not examine mural cell coverage in normal carotid or femoral arteries, hindering the extrapolation of our results to other arteries. Nonetheless, the phenomenon of thin-walled microvessels does not seem to be restricted to coronary arteries.

Because the normal adventitia represents a physiological arterial wall, it is unclear why the morphology of arterial wall angiogenesis differs from the accepted morphology of physiological angiogenesis. Microvessel morphology is generally adapted to local tissue demand, suggesting that mural cells are dispensable in arterial wall angiogenesis. SMC coverage provides vessel stabilization, possibly preventing microvessel compression in situations of high tissue pressure. A recent review described the mathematical theory of arterial wall and microvessel stress in relation to angiogenic perfusion and compression (23). High arterial wall stress, determined by arterial lumen pressure, and low microvessel lumen pressure may lead to the transient (cardiac cycle–dependent) compression of microvessels surrounded by loose structures. Arterial wall stress decreases sharply close to the adventitia according to the Lamé law (23). This relatively low adventitial stress might reduce compression, suggesting that the presence of SMCs in the arterial adventitia is dispensable.

This still does not explain the absence of mural cells in intraplaque angiogenesis. Intraplaque microvessel stress is determined by low microvessel flow and a pressure decrease from the adventitia. Because microvessel diameters are similar in the adventitia and plaque (J. C. Sluimer, unpublished observations, January 2008), however, the pressure decrease from the adventitia to the plaque may be limited (24). Thus, unchanged intraplaque microvessel stress and higher plaque stress suggest that mural cells are necessary to withstand compression, and yet they are absent. Because plaque microvessel stress and flow are currently unknown, their association with mural cell coverage remains to be established.

Infrequent mural cell coverage may also be explained by ongoing or inadequate mural cell recruitment. Ongoing recruitment seems unlikely because pericytes were recruited within 2 weeks in a corneal angiogenesis model (25),

whereas angiogenesis associated with atherosclerotic progression is likely a matter of decades. In addition, ECs in microvessels are not (or no longer) proliferating or apoptotic (19,26). Although pericytes (20) and their recruitment signals have previously been shown in human and mouse atherosclerosis (27,28), inadequate mural cell recruitment to intraplaque angiogenesis has not yet been investigated in vivo.

Perhaps the origin of microvascular leakage is not mural cell coverage but the compromised EC morphology and integrity shown by electron microscopy. The findings in this study are not likely to be caused by artifacts of electron microscopy analysis, because electron microscopy is generally able to detect intact microvessel junctions in several species, tissues, and biopsy sources (29,30). Moreover, the morphology of cells surrounding the microvessels appeared healthy, suggestive of successful tissue collection. Importantly, a previous report showed that reduced expression of the adherens junction marker VE-cadherin in plaque microvessels coincided with open junctions, substantiating the validity of our morphological electron microscopy results (31).

The strikingly deviant EC morphology has also been observed for large artery endothelium at the initiation of atherosclerosis and in hyperglycemic conditions, whereas interendothelial junctions between arterial ECs appeared intact (32). The increased malfunction of intraplaque microvascular compared with arterial endothelium is likely explained by the amplified inflammatory and angiogenic response in advanced compared with early plaques, which may stimulate microvascular permeability.

An important factor determining microvascular permeability is vascular endothelial growth factor (VEGF) (33). The VEGF and its key stimulus hypoxia initiate angiogenesis by disrupting endothelial junctions (34), and both hypoxia and VEGF are present throughout atherogenesis (19). A chronic VEGF stimulus might be involved in the aberrant integrity of microvascular ECs and microvascular leakage. The ECs in microvessels require mural cells to exert an adequate barrier function. The abnormal EC morphology and missing EC junctions may also be caused by the absence of pericytes, as shown in the platelet-derived growth factor B (PDGFB$^{-/-}$) and the PDGF-receptor $\beta^{-/-}$ mouse with failed pericyte recruitment and EC blebbing (35). Actually, these mice also showed increased VEGF expression and decreased capillary perfusion as a result of ECs protruding into and possibly blocking the lumen (36). This suggests compromised microvessel blood flow and increased plaque hypoxia.

In addition, enlarged gaps between ECs and EC blebbing are associated with inflammation and reactive oxygen species, produced by macrophages in atherosclerotic plaques (37,38). Previous studies (39) as well as our electron microscopy images show macrophage–microvessel adhesion and transmigration. In addition, macrophage accumulation in the proximity of intraplaque microvessels and increased adhesion molecule expression on microvascular endothelium (40) are suggestive of macrophage infiltration from permeable microvessels. Also, junctional adhesion molecules enhance macrophage transmigration, and junctional adhesion molecule expression in turn is stimulated by inflammatory infiltration (41). Altogether, we propose that macrophages may not only originate from intraplaque microvessels, but after extravasation may further aggravate microvascular leakage.

Conclusions

MVD is associated with plaque progression and morphology. Microvessel mural cell coverage is incomplete in normal and atherosclerotic human coronary arteries, and is thus unlikely to account for microvascular leakage. However, microvascular leakage may be explained by the compromised structural integrity of intraplaque angiogenesis, and this leaky morphology may explain the extensive leukocyte infiltration, intraplaque hemorrhage, and plaque instability.

Acknowledgments
The authors thank Lila Adams, Hedwig Avalone, and Michael Cooper for excellent technical assistance and Rob Reneman and Arnold Hoeks for stimulating discussions.

Reprint requests and correspondence: Dr. Mat J. A. P. Daemen, Maastricht University Medical Center, Department of Pathology, P.O. Box 5800, 6202 AZ Maastricht, the Netherlands. E-mail: Mat.Daemen@path.unimaas.nl.

REFERENCES

1. Moreno PR, Purushothaman KR, Fuster V, et al. Plaque neovascularization is increased in ruptured atherosclerotic lesions of human aorta: implications for plaque vulnerability. Circulation 2004;110:2032–8.
2. Virmani R, Kolodgie FD, Burke AP, et al. Atherosclerotic plaque progression and vulnerability to rupture angiogenesis as a source of intraplaque hemorrhage. Arterioscler Thromb Vasc Biol 2005;25:2054–61.
3. Bot I, de Jager SC, Zernecke A, et al. Perivascular mast cells promote atherogenesis and induce plaque destabilization in apolipoprotein E-deficient mice. Circulation 2007;115:2516–25.
4. Kockx MM, Cromheeke KM, Knaapen MW, et al. Phagocytosis and macrophage activation associated with hemorrhagic microvessels in human atherosclerosis. Arterioscler Thromb Vasc Biol 2003;23:440–6.
5. Kolodgie FD, Gold HK, Burke AP, et al. Intraplaque hemorrhage and progression of coronary atheroma. N Engl J Med 2003;349:2316–25.
6. de Nooijer R, Verkleij CJ, von der Thusen JH, et al. Lesional overexpression of matrix metalloproteinase-9 promotes intraplaque hemorrhage in advanced lesions but not at earlier stages of atherogenesis. Arterioscler Thromb Vasc Biol 2006;26:340–6.
7. Virmani R, Narula J, Farb A. When neoangiogenesis ricochets. Am Heart J 1998;136:937–9.
8. Carmeliet P, Jain RK. Angiogenesis in cancer and other diseases. Nature 2000;407:249–57.
9. Hashizume H, Baluk P, Morikawa S, et al. Openings between defective endothelial cells explain tumor vessel leakiness. Am J Pathol 2000;156:1363–80.
10. Jain RK. Molecular regulation of vessel maturation. Nat Med 2003;9:685–93.

11. Dejana E. Endothelial cell-cell junctions: happy together. Nat Rev Mol Cell Biol 2004;5:261–70.
12. Virmani R, Kolodgie FD, Burke AP, Farb A, Schwartz SM. Lessons from sudden coronary death: a comprehensive morphological classification scheme for atherosclerotic lesions. Arterioscler Thromb Vasc Biol 2000;20:1262–75.
13. Kolodgie FD, Burke AP, Skorija KS, et al. Lipoprotein-associated phospholipase A2 protein expression in the natural progression of human coronary atherosclerosis. Arterioscler Thromb Vasc Biol 2006; 26:2523–9.
14. Kumamoto M, Nakashima Y, Sueishi K. Intimal neovascularization in human coronary atherosclerosis: its origin and pathophysiological significance. Hum Pathol 1995;26:450–6.
15. Abramsson A, Berlin O, Papayan H, Paulin D, Shani M, Betsholtz C. Analysis of mural cell recruitment to tumor vessels. Circulation 2002;105:112–7.
16. Fleiner M, Kummer M, Mirlacher M, et al. Arterial neovascularization and inflammation in vulnerable patients: early and late signs of symptomatic atherosclerosis. Circulation 2004;110:2843–50.
17. Lappalainen H, Laine P, Pentikainen MO, Sajantila A, Kovanen PT. Mast cells in neovascularized human coronary plaques store and secrete basic fibroblast growth factor, a potent angiogenic mediator. Arterioscler Thromb Vasc Biol 2004;24:1880–5.
18. Khurana R, Simons M, Martin JF, Zachary IC. Role of angiogenesis in cardiovascular disease: a critical appraisal. Circulation 2005;112: 1813–24.
19. Sluimer JC, Gasc JM, van Wanroij JL, et al. Hypoxia, hypoxia-inducible transcription factor, and macrophages in human atherosclerotic plaques are correlated with intraplaque angiogenesis. J Am Coll Cardiol 2008;51:1258–65.
20. Liu Y, Wilkinson FL, Kirton JP, et al. Hepatocyte growth factor and c-Met expression in pericytes: implications for atherosclerotic plaque development. J Pathol 2007;212:12–9.
21. Dunmore BJ, McCarthy MJ, Naylor AR, Brindle NP. Carotid plaque instability and ischemic symptoms are linked to immaturity of microvessels within plaques. J Vasc Surg 2007;45:155–9.
22. Mazzone A, Epistolato MC, Gianetti J, et al. Biological features (inflammation and neoangiogenesis) and atherosclerotic risk factors in carotid plaques and calcified aortic valve stenosis: two different sites of the same disease? Am J Clin Pathol 2006;126:494–502.
23. Ritman EL, Lerman A. The dynamic vasa vasorum. Cardiovasc Res 2007;75:649–58.
24. Hoeks AP, Reesink KD, Hermeling E, Reneman RS. Local blood pressure rather than shear stress should be blamed for plaque rupture. J Am Coll Cardiol 2008;52:1107–8.
25. Cursiefen C, Hofmann-Rummelt C, Kuchle M, Schlotzer-Schrehardt U. Pericyte recruitment in human corneal angiogenesis: an ultrastructural study with clinicopathological correlation. Br J Ophthalmol 2003;87:101–6.
26. Tricot O, Mallat Z, Heymes C, Belmin J, Leseche G, Tedgui A. Relation between endothelial cell apoptosis and blood flow direction in human atherosclerotic plaques. Circulation 2000;101:2450–3.
27. Pilarczyk K, Sattler KJ, Galili O, et al. Placenta growth factor expression in human atherosclerotic carotid plaques is related to plaque destabilization. Atherosclerosis 2008;196:333–40.
28. Khurana R, Moons L, Shafi S, et al. Placental growth factor promotes atherosclerotic intimal thickening and macrophage accumulation. Circulation 2005;111:2828–36.
29. Luksha L, Poston L, Gustafsson JA, Hultenby K, Kublickiene K. The oestrogen receptor beta contributes to sex related differences in endothelial function of murine small arteries via EDHF. J Physiol 2006;577:945–55.
30. Baloyannis SJ. Pathological alterations of the climbing fibres of the cerebellum in vascular dementia: a Golgi and electron microscope study. J Neurol Sci 2007;257:56–61.
31. Bobryshev YV, Cherian SM, Inder SJ, Lord RS. Neovascular expression of VE-cadherin in human atherosclerotic arteries and its relation to intimal inflammation. Cardiovasc Res 1999;43:1003–17.
32. Simionescu M, Popov D, Sima A, et al. Pathobiochemistry of combined diabetes and atherosclerosis studied on a novel animal model. The hyperlipemic-hyperglycemic hamster. Am J Pathol 1996; 148:997–1014.
33. van Hinsbergh VW, van Nieuw Amerongen GP. Intracellular signalling involved in modulating human endothelial barrier function. J Anat 2002;200:549–60.
34. Suarez S, Ballmer-Hofer K. VEGF transiently disrupts gap junctional communication in endothelial cells. J Cell Sci 2001;114:1229–35.
35. Hellstrom M, Gerhardt H, Kalen M, et al. Lack of pericytes leads to endothelial hyperplasia and abnormal vascular morphogenesis. J Cell Biol 2001;153:543–53.
36. Gerhardt H, Betsholtz C. Endothelial-pericyte interactions in angiogenesis. Cell Tissue Res 2003;314:15–23.
37. Hazell LJ, Arnold L, Flowers D, Waeg G, Malle E, Stocker R. Presence of hypochlorite-modified proteins in human atherosclerotic lesions. J Clin Invest 1996;97:1535–44.
38. McDonald DM, Thurston G, Baluk P. Endothelial gaps as sites for plasma leakage in inflammation. Microcirculation 1999;6:7–22.
39. Balakrishnan KR, Kuruvilla S. Images in cardiovascular medicine. Role of inflammation in atherosclerosis: immunohistochemical and electron microscopic images of a coronary endarterectomy specimen. Circulation 2006;113:e41–3.
40. O'Brien KD, McDonald TO, Chait A, Allen MD, Alpers CE. Neovascular expression of E-selectin, intercellular adhesion molecule-1, and vascular cell adhesion molecule-1 in human atherosclerosis and their relation to intimal leukocyte content. Circulation 1996;93:672–82.
41. Weber C, Fraemohs L, Dejana E. The role of junctional adhesion molecules in vascular inflammation. Nat Rev Immunol 2007;7:467–77.

Key Words: coronary atherosclerosis ■ angiogenesis ■ microvascular leakage ■ junctions ■ ultrastructure.